

Reaction Mechanisms of Metal–Metal-bonded Carbonyls. Part 19.¹ Homolytic Fission of Bis[tetracarbonyl(triphenylphosphine)manganese]-(Mn–Mn) as a Path for Thermal Substitution²

By J. Paul Fawcett, Ronald A. Jackson, and Anthony Poë,* Erindale College and the Department of Chemistry, University of Toronto, Mississauga, Ontario L5L 1C6, Canada

The complex $[\{\text{Mn}(\text{CO})_4(\text{PPh}_3)_2\}]$ reacts with $\text{P}(\text{OPh})_3$ in cyclohexane at 40–50 °C to form $[\text{Mn}_2(\text{CO})_8(\text{PPh}_3)_2\text{P}(\text{OPh})_3]$. A detailed study of the dependence of the rate on the concentrations of complex, $\text{P}(\text{OPh})_3$, and PPh_3 shows that the kinetics are fully consistent with a mechanism involving initial, reversible, homolytic fission. This is followed by reversible bimolecular substitution of PPh_3 in $[\text{Mn}(\text{CO})_4(\text{PPh}_3)]$ by $\text{P}(\text{OPh})_3$ before final formation of the product by combination of two unlike radicals. This is the first clearly demonstrated example of a mechanism of this type operating in a simple thermal-substitution reaction.

Thermal reactions of $[\text{M}_2(\text{CO})_{10}]$ ($\text{M}_2 = \text{Mn}_2$,³ MnRe ,³ Tc_2 ,⁴ or Re_2 ,⁵) and $[\{\text{Mn}(\text{CO})_4[\text{P}(\text{OPh})_3]_2\}]$ ⁶ with oxygen in decalin show kinetic behaviour indicative of reversible homolytic fission as the initial step that leads to eventual decomposition. The half-order dependence on [complex] of the thermal decomposition of the complexes $[\{\text{Mn}(\text{CO})_4[\text{P}(\text{OPh})_3]_2\}]$ ⁶ and $[\{\text{Re}(\text{CO})_4(\text{PPh}_3)_2\}]$ ⁷ in decalin under argon and in the presence of an excess of $\text{P}(\text{OPh})_3$ and PPh_3 , respectively, provides similar evidence as does the formation¹ of *cis*- $[\text{Mn}(\text{CO})_4(\text{L})\text{Cl}]$ [$\text{L} = \text{PPh}_3$, PBU_3 , or $\text{P}(\text{C}_6\text{H}_{11})_3$] on reaction of $[\{\text{Mn}(\text{CO})_4\text{L}\}_2]$ with *sym*- $\text{C}_2\text{H}_2\text{Cl}_4$. Recently Benner and Balch⁸ have qualitatively demonstrated that thermal homolytic fission occurs in several such complexes by spin trapping of the radicals produced. Substitution reactions of some of these complexes have kinetic parameters very similar to, although not always identical with, those for reaction with O_2 and it has been concluded that homolytic fission plays a major role in these substitutions.¹ We present here detailed kinetic evidence showing that thermal-substitution reactions of $[\{\text{Mn}(\text{CO})_4(\text{PPh}_3)_2\}]$ with $\text{P}(\text{OPh})_3$ or CO also proceed *via* initial homolytic fission.² A partial study of these reactions was reported first by Wawersik and Basolo.⁹

EXPERIMENTAL AND RESULTS

The preparation of the complex $[\{\text{Mn}(\text{CO})_4(\text{PPh}_3)_2\}]$, the chemicals used, and the kinetic procedures followed have all been described elsewhere.¹⁰ Certified Grade A.C.S. cyclohexane (Fisher Scientific Co.) was stored over molecular sieves and used without further purification. The complex showed bands in the i.r. at 1 987w and 1 963 cm^{-1} (ϵ $22 \times 10^3 \text{ dm}^3 \text{ mol}^{-1} \text{ cm}^{-1}$), and has an absorption maximum at 376 nm (ϵ $3.2 \times 10^4 \text{ dm}^3 \text{ mol}^{-1} \text{ cm}^{-1}$) in its electronic spectrum together with a shoulder at 440 nm. These data are in good agreement with those published elsewhere.^{1,11} Reaction with an excess of $\text{P}(\text{OPh})_3$ at 50 °C in cyclohexane was accompanied by growth of i.r.

bands at 1 988w, 1 974s, and 1 928w cm^{-1} , and by corresponding loss of the band at 1 963 cm^{-1} due to the reactant complex. The product had an absorption maximum at 367 nm (ϵ $2 \times 10^4 \text{ dm}^3 \text{ mol}^{-1} \text{ cm}^{-1}$) in its electronic spectrum, with a shoulder at *ca.* 425 nm. An isolated sample of $[\{\text{Mn}(\text{CO})_4[\text{P}(\text{OPh})_3]_2\}]$ had i.r. absorption bands in cyclohexane at 2 004w and 1 983 cm^{-1} (ϵ $16 \times 10^3 \text{ dm}^3 \text{ mol}^{-1} \text{ cm}^{-1}$) and an electronic-absorption band at 355 nm with a shoulder at 408 nm.⁶ When the product of the reaction of $[\{\text{Mn}(\text{CO})_4(\text{PPh}_3)_2\}]$ (*ca.* $4 \times 10^{-4} \text{ mol dm}^{-3}$) with $\text{P}(\text{OPh})_3$ (0.10 mol dm^{-3}) in cyclohexane at 50 °C was heated to 75 °C the band at 1 974 cm^{-1} slowly disappeared, to be replaced by the band at 1 983 cm^{-1} characteristic of $[\{\text{Mn}(\text{CO})_4[\text{P}(\text{OPh})_3]_2\}]$. The final yield of this complex, however, was only *ca.* 20%. Reaction of the bis(phosphine) complex with 0.05 mol dm^{-3} $\text{P}(\text{OPh})_3$ at 50 °C under argon in a silica cell was followed by repetitive scanning in a Perkin-Elmer 402 recording spectrophotometer. Reasonable isosbestic points were observed at *ca.* 350 and *ca.* 425 nm which persisted up to *ca.* 50% completion of reaction, after which there was a general decrease in absorbance. The decrease was probably due to leakage of O_2 into the cell which could not be as tightly sealed as the Schlenk tubes. These results show that the reaction of $[\{\text{Mn}(\text{CO})_4(\text{PPh}_3)_2\}]$ with $\text{P}(\text{OPh})_3$ leads first to the formation of the mixed complex $[\text{Mn}_2(\text{CO})_8(\text{PPh}_3)_2\text{P}(\text{OPh})_3]$ for which the molar absorption coefficient at 1 974 cm^{-1} was estimated to be $12 \times 10^3 \text{ dm}^3 \text{ mol}^{-1} \text{ cm}^{-1}$.

The kinetics of the reaction were followed by monitoring the decreasing intensity of the band at 1 963 cm^{-1} . The molar absorption coefficients of $[\text{Mn}_2(\text{CO})_8(\text{PPh}_3)_2\text{P}(\text{OPh})_3]$, $\text{P}(\text{OPh})_3$, and PPh_3 at this frequency are 1.9×10^3 , 2.3, and 7.2 $\text{dm}^3 \text{ mol}^{-1} \text{ cm}^{-1}$, respectively, and the absorbances, A_∞ , of the reaction mixtures at completion of reaction were calculated from these values and the known concentrations. In all cases the reactions went to completion. In the absence of free PPh_3 , first-order rate plots were found to be linear for *ca.* 2 half-lives when $[\text{P}(\text{OPh})_3] = 0.190 \text{ mol dm}^{-3}$ and the initial concentration of complex was 7.1×10^{-5} – $36.5 \times 10^{-5} \text{ mol dm}^{-3}$. The first-order rate constants were independent of complex concentration. When $[\text{P}(\text{OPh})_3] = 0.010 \text{ mol dm}^{-3}$, however, the first-order

¹ Part 18, R. A. Jackson and A. J. Poe, *Inorg. Chem.*, 1978, **17**, in the press.

² J. P. Fawcett, R. A. Jackson, and A. J. Poë, *J.C.S. Chem. Comm.*, 1975, 733.

³ J. P. Fawcett, A. J. Poë, and K. R. Sharma, *J. Amer. Chem. Soc.*, 1976, **98**, 1401.

⁴ J. P. Fawcett and A. J. Poë, *J.C.S. Dalton*, 1976, 2039.

⁵ A. J. Poë and K. R. Sharma, unpublished work.

⁶ D. M. Chowdhury, A. J. Poë, and K. R. Sharma, *J.C.S. Dalton*, 1977, 2352.

⁷ D. G. DeWit, J. P. Fawcett, and A. J. Poë, *J.C.S. Dalton*, 1976, 528.

⁸ L. S. Benner and A. L. Balch, *J. Organometallic Chem.*, 1977, **134**, 121.

⁹ H. Wawersik and F. Basolo, *Inorg. Chim. Acta*, 1969, **3**, 113.

¹⁰ J. P. Fawcett and A. J. Poë, *J.C.S. Dalton*, 1977, 1302.

¹¹ R. A. Levenson and H. B. Gray, *J. Amer. Chem. Soc.*, 1975, **97**, 6042.

rate plots showed pronounced curvature, the gradients increasing with time. Apparent first-order rate constants, k_{obs} , can be defined by the equation $R = k_{\text{obs}}c$ where R represents the rate at a particular concentration, c , of

TABLE 1

Dependence on [complex] of the apparent first-order rate constants for reaction of P(OPh)_3 with $\{[\text{Mn}(\text{CO})_4(\text{PPh}_3)_2]\}$ in cyclohexane in the absence of PPh_3

$10^3 c^a$ mol dm ⁻³	$10^6 k_{\text{obs.}}$ s ⁻¹	$10^6 k_{\text{calc.}}^b$ s ⁻¹	$\frac{\Delta c}{\%}$
(a) 39.9 °C, $[\text{P(OPh)}_3] = 0.010 \text{ mol dm}^{-3}$			
16.4	24.9	25.3	-1.7
21.8	22.9	23.2	-1.4
25.3	24.6	21.9	11.1
29.0	22.3	21.2	5.2
46.6	17.3	18.0	-3.8
47.5	18.0	17.9	0.7
47.9	18.8	17.8	5.7
50.2	16.7	17.5	-4.6
99.7	12.3	13.4	-8.2
113	10.6	12.7	-16.7
134	12.3	11.8	3.8
160	10.8	11.0	-1.7
184	10.3	10.4	-1.0
189	10.3	10.3	0
196	9.01	10.1	-10.9
240	8.52	9.25	-7.9
329	8.39	8.02	4.6
360	7.80	7.72	1.0
(b) 38.0 °C, $[\text{P(OPh)}_3] = 0.190 \text{ mol dm}^{-3}$			
70.7	315		} $10^6 k_{\text{obs.}} = 325 \pm 6$
162	328		
211	325		
261	320		
365	339		

^a Concentration of $\{[\text{Mn}(\text{CO})_4(\text{PPh}_3)_2]\}$. ^b By using $k_1 = 4.20 \times 10^{-4} \text{ s}^{-1}$ and $k_{-1}^{\ddagger}/k_2 = 126 \text{ mol}^{\ddagger} \text{ dm}^{-\ddagger} \text{ s}^{\ddagger}$. ^c $100 (k_{\text{obs.}} - k_{\text{calc.}})/k_{\text{calc.}}$.

complex. A zero subscript can be added to R to give R_0 , the rate in the absence of added PPh_3 . We chose, for convenience, to measure c at the beginning of each reaction from the initial absorbance, the known molar absorption

TABLE 2

Dependence on $[\text{P(OPh)}_3]$ of the apparent first-order rate constants in the absence of PPh_3 at 49.9 °C

$10^3 [\text{P(OPh)}_3]$ mol dm ⁻³	$10^6 c$ mol dm ⁻³	$10^5 k_{\text{obs.}}$ s ⁻¹	$10^5 k_{\text{calc.}}^*$ s ⁻¹	$\frac{\Delta}{\%}$
10.4	300	38.0	37.9	0.3
12.9	274	51.2	47.4	8.0
15.4	265	57.6	55.7	3.4
20.4	274	66.5	68.6	-3.1
30.0	309	83.8	86.6	-3.2
48.5	315	113	115	-1.7
84.8	328	139	143	-2.8
173	294	169	167	1.2

* By using $k_1 = 176 \times 10^{-5} \text{ s}^{-1}$ and $k_{-1}/k_2^2 = 35 \times 10^2 \text{ mol dm}^{-3} \text{ s}$.

coefficient, and the path length of the cell. The corresponding values of k_{obs} , (and, therefore, of R_0 or R) were obtained from the initial gradients of the first-order plots.

Values of k_{obs} showed a strong dependence on c at $[\text{P(OPh)}_3] = 0.010 \text{ mol dm}^{-3}$, $[\text{PPh}_3] = 0 \text{ mol dm}^{-3}$, and $c = 1.64 \times 10^{-5}$ — $36.0 \times 10^{-5} \text{ mol dm}^{-3}$. A plot of $\log R_0$ against $\log c$ was curved (Figure 1, ref. 2) with a gradient significantly less than unity even at low values of c . Rates

were also measured for $c = ca. 3 \times 10^{-4} \text{ mol dm}^{-3}$ and various concentrations of P(OPh)_3 and PPh_3 . The values of k_{obs} were found to increase to a limiting value with increasing $[\text{P(OPh)}_3]$ (as was observed earlier),⁹ and to decrease with increasing $[\text{PPh}_3]$. All the kinetic data are shown in Tables 1—3.

TABLE 3

Dependence on $[\text{PPh}_3]$ and $[\text{P(OPh)}_3]$ of the apparent first-order rate constants at 49.9 °C

$10^3 [\text{PPh}_3]$ mol dm ⁻³	$10^3 [\text{P(OPh)}_3]$ mol dm ⁻³	$10^6 c$ mol dm ⁻³	$10^4 k_{\text{obs.}}$ s ⁻¹	$10^5 k_{\text{calc.}}^*$ s ⁻¹	$\frac{\Delta}{\%}$
1.28	18.0	228	57.0	66.2	-14
5.01	18.0	282	53.2	56.9	-6.5
10.0	18.0	387	47.4	46.9	1.1
22.2	18.0	296	42.3	42.8	-1.2
42.4	18.0	296	30.8	33.9	-9.1
95.5	18.2	330	20.8	22.0	-5.5
31.2	9.24	276	22.1	21.7	1.8
31.2	10.1	219	24.8	24.9	-0.4
31.2	14.2	286	32.4	31.6	2.5
31.2	18.2	260	41.6	39.6	5.1
32.4	28.8	272	61.3	55.7	10.1
31.2	45.6	246	82.6	78.7	5.0
31.2	50.7	182	90.7	87.5	3.7
31.6	100	254	111	116	-4.3
31.2	102	168	117	121	-3.3
31.1	156	330	143	133	7.5

* By using $k_1 = 175 \times 10^{-5} \text{ s}^{-1}$, $k_{-1}^{\ddagger}/k_2 = 57 \text{ mol}^{\ddagger} \text{ dm}^{-\ddagger} \text{ s}^{\ddagger}$, and $k_{-1}k_{-2}/k_2k_3 = 0.9$.

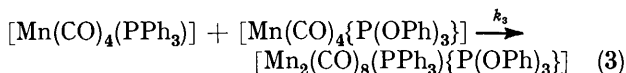
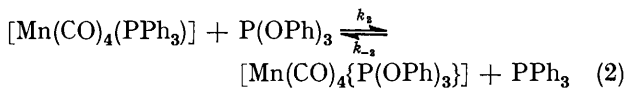
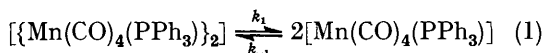
DISCUSSION

The curvature and less-than-unit gradient of the plot of $\log R_0$ against $\log c$ when $[\text{P(OPh)}_3] = 0.010 \text{ mol dm}^{-3}$ is characteristic^{3-6,12} of initial reversible fission of the complex into two fragments, further reaction of the fragments competing with their recombination. The rate of this further reaction must, in this case, be dependent on $[\text{P(OPh)}_3]$ since the values of k_{obs} increase with $[\text{P(OPh)}_3]$ to a limiting value. Under this limiting condition the reaction is strictly first order in [complex] and the rate-determining step is the fission process, no recombination of fragments occurring. It is most unlikely that the fission process is heterolytic since the ions formed would be tightly bound in an ion pair in such a non-polar solvent as cyclohexane. The reformation of the binuclear complex would then be first order in [ion pair] and the overall kinetics would remain first order in [complex] at all concentrations. An unsymmetrical distribution of ligands between the two fragments can also be concluded to be most unlikely on energetic grounds, one fragment being co-ordinatively oversaturated and the other unsaturated. Since the product of the reaction corresponds to substitution of only one PPh_3 ligand, the qualitative nature of the data therefore suggests the reaction scheme shown in equations (1)—(3). The reversibility of reaction (2) is shown by the retarding effect of free PPh_3 , and the irreversibility of (3) by the fact that the reaction goes to completion under all conditions used.

In the absence of free PPh_3 , (2) can be considered irreversible and rate equations (8) and (9) can be derived

¹² J. P. Fawcett, A. J. Poë, and M. V. Twigg, *J. Organometallic Chem.*, 1973, **51**, C17.

as follows by using the steady-state approximation. R_1 represents the rate of reaction (1) in the forward direction, and R_0 the corresponding observed rate.



$\text{M} = \text{Mn}(\text{CO})_4$, $\text{L} = \text{PPh}_3$, $\text{L}' = \text{P}(\text{OPh})_3$, and $[\text{ML}]_0$ and $[\text{ML}']_0$ represent the steady-state concentrations of these intermediates. The steady state is assumed to be set up very rapidly, *i.e.* k_{-1} and k_2 are much greater than k_1 . From (4) and (6) we obtain (7), and from (4) and (7) we obtain (8) or (9). A plot of k_{obs} against

$$R_0 = k_1[(\text{ML})_2] - k_{-1}[\text{ML}]_0^2 = k_3[\text{ML}]_0[\text{ML}']_0 \quad (4)$$

$$2k_1[(\text{ML})_2] - 2k_{-1}[\text{ML}]_0^2 - k_2[\text{ML}]_0[\text{L}'] - k_3[\text{ML}]_0[\text{ML}']_0 = 0 \quad (5)$$

$$k_2[\text{ML}]_0[\text{L}'] - k_3[\text{ML}]_0[\text{ML}']_0 = 0 \quad (6)$$

$$[\text{ML}]_0 = R_0/k_2[\text{L}'] \quad (7)$$

$$(R_1 - R_0)^{1/2}[\text{L}']/R_0 = k_{-1}^{1/2}/k_2 \quad (8)$$

$$R_0/c = k_{\text{obs}} = k_1 - (k_{-1}/k_2^2)(R_0^2/c[\text{L}']^2) \quad (9)$$

$R_0^2/c[\text{P}(\text{OPh})_3]^2$ for reaction with $[\text{P}(\text{OPh})_3]$ at 49.9 °C (Table 2) is shown in Figure 1. The deviations of the

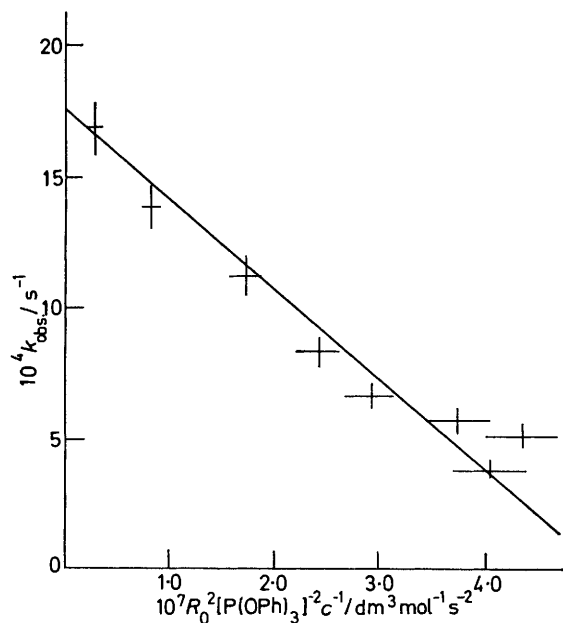


FIGURE 1 Dependence of k_{obs} on $[\text{P}(\text{OPh})_3]$ for reaction at 49.9 °C, $[\text{PPh}_3] = 0$, and $c = 3 \times 10^{-4} \text{ mol dm}^{-3}$

values of k_{obs} from those calculated with parameters given by the line drawn in the Figure correspond to a standard deviation, $\sigma(k_{\text{obs}})$, for each individual measure-

ment of k_{obs} of 5.5%, after allowing for the number of degrees of freedom. The uncertainties shown for each point in the Figure correspond to this standard deviation. The values of k_1 and k_{-1}/k_2^2 obtained from the graph are

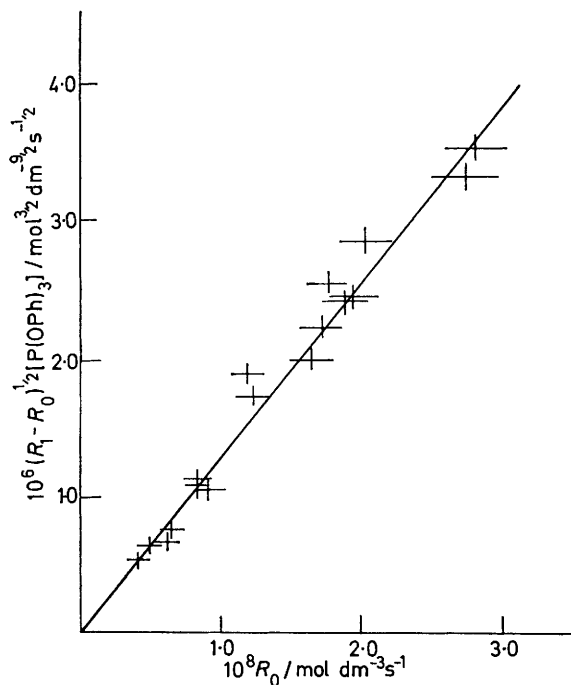


FIGURE 2 Dependence of rate on $[\text{complex}]$ for reaction with $0.010 \text{ mol dm}^{-3} \text{ P}(\text{OPh})_3$ at 39.9 °C, $[\text{PPh}_3] = 0$, and $c = 2 \times 10^{-4} - 36 \times 10^{-4} \text{ mol dm}^{-3}$

$(175 \pm 8) \times 10^{-5} \text{ s}^{-1}$ and $(35 \pm 7) \times 10^2 \text{ mol dm}^{-3} \text{ s}$, respectively. The uncertainties are approximate estimates of the standard deviations made by drawing two reasonable extreme linear plots and assuming that the parameters obtained from them are reasonable estimates of the 95% confidence limits. This value of k_1 at 49.9 °C is in excellent agreement with the value $(175 \pm 2) \times 10^{-5} \text{ s}^{-1}$ estimated from the activation parameters for reaction of the complex with carbon monoxide.¹⁰ The value $k_1 = (325 \pm 6) \times 10^{-6} \text{ s}^{-1}$ obtained from the reaction with $0.190 \text{ mol dm}^{-3} \text{ P}(\text{OPh})_3$ at 38.0 °C (Table 1) is also in excellent agreement with the value $(317 \pm 7) \times 10^{-6} \text{ s}^{-1}$ estimated for reaction with carbon monoxide at that temperature.⁹ The limiting first-order rate constants for reaction with $\text{P}(\text{OPh})_3$ and CO are therefore identical over this temperature range and both reactions must proceed by the same rate-determining step. A value of $k_1 = (420 \pm 9) \times 10^{-6} \text{ s}^{-1}$ for reaction with CO at 39.9 °C can be calculated from the activation parameters¹⁰ and this can be used to calculate values of R_1 for reaction with $\text{P}(\text{OPh})_3$ at that temperature. It is, therefore, possible to calculate values of $(R_1 - R_0)^{1/2}[\text{P}(\text{OPh})_3]$ for reaction with $0.010 \text{ mol dm}^{-3} \text{ P}(\text{OPh})_3$ at 39.9 °C (Table 1) and these values are plotted against corresponding values of R_0 in Figure 2. A straight line passing through the origin is easily drawn through the points in accordance

with equation (8). The deviations of R_0 from the line drawn lead to a value of $\pm 7.6\%$ for $\sigma(k_{\text{obs.}})$ and the uncertainties indicated for the points are standard deviations based on this value and on the uncertainty for k_1 . The gradient of the plot leads to a value of $126 \pm 7 \text{ mol}^{\frac{1}{2}} \text{ dm}^{-\frac{3}{2}} \text{ s}^{\frac{1}{2}}$ for $k_{-1}^{\frac{1}{2}}/k_2$ at 39.9°C , the uncertainty being an approximate standard deviation estimated as before.

For reaction in the presence of free PPh_3 , rate equation (13) can be derived as follows. $[\text{ML}]$ and $[\text{ML}']$ represent the steady-state concentrations of these intermediates under these conditions and R is the observed

The value for the enthalpy difference is much greater than the 15 kJ mol^{-1} found³ from the reaction of $[\text{Mn}(\text{CO})_{10}]$ with O_2 . Although the recombination of two $[\text{Mn}(\text{CO})_4(\text{PPh}_3)]$ radicals would be expected to have a somewhat higher activation enthalpy than recombination of two $[\text{Mn}(\text{CO})_5]$ radicals, bimolecular substitution of PPh_3 in $[\text{Mn}(\text{CO})_4(\text{PPh}_3)]$ by $\text{P}(\text{OPh})_3$ would have a very much higher value of ΔH^\ddagger than would reaction of O_2 with $[\text{Mn}(\text{CO})_5]$.

The fact that $\text{P}(\text{OPh})_3$ displaces PPh_3 from $[\text{Mn}(\text{CO})_4(\text{PPh}_3)]$ by a bimolecular mechanism, rather than by

TABLE 4

Rate parameters for the mechanism shown in equations (1)–(3)

θ_c $^\circ \text{C}$	$\frac{10^5 c}{\text{mol dm}^{-3}}$	$\frac{10^3 [\text{P}(\text{OPh})_3]}{\text{mol dm}^{-3}}$	$\frac{10^3 [\text{PPh}_3]}{\text{mol dm}^{-3}}$	$\frac{10^5 k_1}{\text{s}^{-1}}$	$\frac{10^{-2} (k_{-1}/k_2^2)}{\text{mol dm}^{-3} \text{ s}}$	$\frac{k_{-1} k_{-2}}{k_2 k_3}$
38.0	7–37	190	0	32.5 ± 0.6		
	32	0	0	$31.7 \pm 0.7^*$		
39.9	2–36	10	0	$42.0 \pm 0.9^*$	159 ± 10	
49.9	27–32	10–173	0	175 ± 8	35 ± 7	
	18–39	9–156	1–96	$175 \pm 2^*$	33 ± 10	0.9 ± 0.1

* Calculated from activation parameters¹⁰ for reaction with CO.

rate. A plot of $(R_1 - R)^{\frac{1}{2}}[\text{P}(\text{OPh})_3]/R$ against $[\text{PPh}_3]/(R_1 - R)^{\frac{1}{2}}$ is shown in Figure 3. Values of R were

$$R = k_1[(\text{ML})_2] - k_{-1}[\text{ML}]^2 \quad (10)$$

$$2k_1[(\text{ML})_2] - 2k_{-1}[\text{ML}]^2 - k_2[\text{ML}][\text{L}'] + k_{-2}[\text{ML}'][\text{L}] - k_3[\text{ML}][\text{ML}'] = 0 \quad (11)$$

$$k_2[\text{ML}][\text{L}'] - k_{-2}[\text{ML}'][\text{L}] - k_3[\text{ML}][\text{ML}'] = 0 \quad (12)$$

whence

$$[\text{ML}] = (R_1 - R)^{\frac{1}{2}}/k_{-1}^{\frac{1}{2}}$$

$$[\text{ML}'] = k_2[\text{ML}][\text{L}']/(k_{-2}[\text{L}] + k_3[\text{ML}])$$

and

$$(R_1 - R)^{\frac{1}{2}}[\text{L}']/R = \frac{(k_{-1}^{\frac{1}{2}}/k_2) + (k_{-1}k_{-2}/k_2k_3)[\text{L}]/(R_1 - R)^{\frac{1}{2}}}{(k_{-1}^{\frac{1}{2}}/k_2) + (k_{-1}k_{-2}/k_2k_3)[\text{L}]/(R_1 - R)^{\frac{1}{2}}} \quad (13)$$

obtained from Table 3 and k_{-1} was taken as $(175 \pm 2) \times 10^{-5} \text{ s}^{-1}$ (see above). The uncertainties in the points are approximate standard deviations based on a value $\sigma(k_{\text{obs.}}) = 7.2\%$ estimated from the differences between $k_{\text{obs.}}$ and $k_{\text{calc.}}$. {Significant uncertainties along the horizontal axis occur only in those cases where $[\text{PPh}_3] = \text{ca. } 0.03 \text{ mol dm}^{-3}$ and $[\text{P}(\text{OPh})_3]$ is high so that R is approaching quite close to R_1 and $(R_1 - R)^{\frac{1}{2}}$ becomes quite uncertain.} Values of $k_{\text{calc.}}$ were derived from the parameters $k_{-1}^{\frac{1}{2}}/k_2 = 57 \pm 7 \text{ mol}^{\frac{1}{2}} \text{ dm}^{-\frac{3}{2}} \text{ s}^{\frac{1}{2}}$ and $k_{-1}k_{-2}/k_2k_3 = 0.9 \pm 0.1$ obtained from the intercept and gradient, respectively, of the linear plot in Figure 3. The uncertainties in these parameters are approximate standard deviations derived as before by drawing reasonable extreme plots. The value of $k_{-1}^{\frac{1}{2}}/k_2$ from these results is in excellent agreement with the value $59 \pm 6 \text{ mol}^{\frac{1}{2}} \text{ dm}^{-\frac{3}{2}} \text{ s}^{\frac{1}{2}}$ found above from the data in Table 2. All the data are therefore qualitatively and quantitatively consistent with each other and with the proposed mechanism (Table 4).

The values of $k_{-1}^{\frac{1}{2}}/k_2$ at 39.9 and 49.9°C enable a value of $129 \pm 10 \text{ kJ mol}^{-1}$ to be estimated for $2\Delta H_{-2}^\ddagger - \Delta H_{-1}^\ddagger$, and $87 \pm 32 \text{ J K}^{-1} \text{ mol}^{-1}$ for $2\Delta S_{-2}^\ddagger - \Delta S_{-1}^\ddagger$.

rate-determining PPh_3 dissociation, is not surprising. The formation of a six-co-ordinate 19-electron transition state during a bimolecular reaction involves the

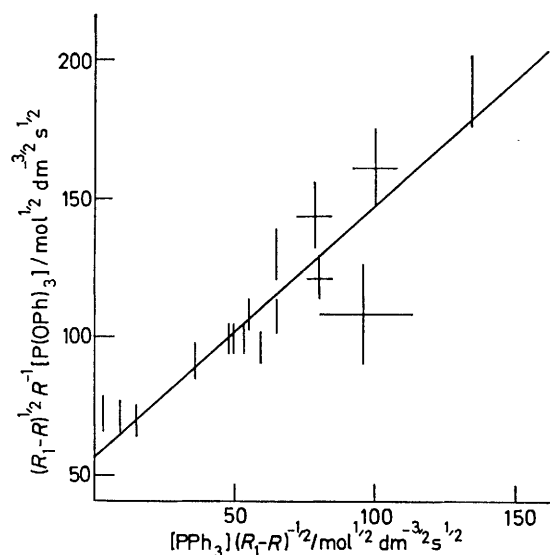
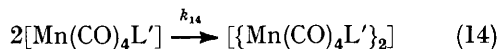


FIGURE 3 Dependence of kinetic behaviour on $[\text{PPh}_3]$ and $[\text{P}(\text{OPh})_3]$ at $c = 1.7 \times 10^{-4}$ – $3.9 \times 10^{-4} \text{ mol dm}^{-3}$

partial formation of an additional 'half-bond' whereas the dissociative mechanism would involve partial breaking of a whole bond. It is, therefore, intermediate between reaction of an 18-electron octahedral complex (where bimolecular reactions are known although not very common) and a 16-electron planar four-co-ordinate complex (where bimolecular reactions are the rule). The fact that the limiting rate is reached at much lower values¹⁰ of $[\text{CO}]$ than of $[\text{P}(\text{OPh})_3]$ implies that bimolecular attack by CO is much more favoured. Attack by PBu_3 ⁹ can be inferred in this way to be intermediate in rate between that by CO and $\text{P}(\text{OPh})_3$ and this

sequence is explicable in terms of the conflicting effects of basicity and size.

The kinetic behaviour is also consistent with the observation that $[\text{Mn}_2(\text{CO})_8(\text{PPh}_3)\{\text{P}(\text{OPh})_3\}]$ is the only product observed. If reaction (3) were replaced by (14)



$$(R_1 - R)^{\ddagger}[\text{L}']/R = \frac{2(k_{-1}^{\ddagger}/k_2) + (k_{-1}^{\ddagger}k_{-2}/k_2k_{14}^{\ddagger})[\text{L}]/R^{\ddagger}}{\quad} \quad (15)$$

rate equation (15) applies. The kinetic form of behaviour will be the same as before when $[\text{PPh}_3] = 0$, but when free PPh_3 is present it should be different. This difference is not pronounced when $[\text{P}(\text{OPh})_3] = \text{constant}$ and $[\text{PPh}_3]$ is varied, the term $[\text{PPh}_3]/R^{\ddagger}$ merely increasing more rapidly with $[\text{PPh}_3]$ than $[\text{PPh}_3]/(R_1 - R)^{\ddagger}$. However, when $[\text{PPh}_3] = \text{constant}$ and $[\text{P}(\text{OPh})_3]$ is varied $[\text{PPh}_3]/R^{\ddagger}$ decreases with increasing $[\text{P}(\text{OPh})_3]$ whereas $[\text{PPh}_3]/(R_1 - R)^{\ddagger}$ increases with $[\text{P}(\text{OPh})_3]$. A negative (and, therefore, meaningless) value is thus found for $(k_{-1}^{\ddagger}k_{-2}/k_2k_{14}^{\ddagger})$ and the intercept is more than twice the value predicted from the data in the absence of added PPh_3 .

The preferential combination of unlike radicals is also

known in other systems. Thus $[\{\text{Re}(\text{CO})_4(\text{PPh}_3)\}_2]$ is also believed to react *via* initial reversible homolytic fission⁷ and reaction with $\text{P}(\text{OPh})_3$ yields $[\text{Re}_2(\text{CO})_8(\text{PPh}_3)\{\text{P}(\text{OPh})_3\}]$ as the primary product. In this case, however, the limiting rate is reached at all concentrations of $\text{P}(\text{OPh})_3$ used (provided $[\text{PPh}_3] = 0$) and R_2 must be $\gg R_1$. A similar preference for reaction between the unlike radicals $[\text{Mn}(\text{CO})_5]$ and $[\text{Re}(\text{CO})_5]$ compared with reaction between like radicals has also been shown in the thermal decomposition of $[\text{MnRe}(\text{CO})_{10}]^3$ and is also suggested³ by photochemical studies.¹³ Substitution reactions of CO with $[\{\text{M}(\text{CO})_4(\text{PPh}_3)\}_2]$ ($\text{M} = \text{Tc}$ or Re) and $[\{\text{Mn}(\text{CO})_4\text{L}\}_2]$ [$\text{L} = \text{P}(\text{OPh})_3$ or $\text{P}(\text{C}_6\text{H}_{11})_3$] are also believed^{1,4,6,7} to react *via* homolytic fission and the initial product in each case is the nonacarbonyl. This shows that the final step is the preferential combination of $[\text{M}(\text{CO})_5]$ and $[\text{M}(\text{CO})_4\text{L}]$ radicals. The cause of this selectivity is not yet clear.

We thank Erindale College and the National Research Council, Ottawa, for support, and the National Research Council for the award of a fellowship (to R. A. J.).

[7/1743 Received, 3rd October, 1977]

¹³ M. S. Wrighton and D. S. Ginley, *J. Amer. Chem. Soc.*, 1975, **97**, 2065.